

ECMM102

Group Project (Meng) (A, TRM1+2 2015/6)

012184



1019571



By submitting coursework you declare that you understand and consent to the University policies regarding plagiarism and mitigation (these can be seen online at www.exeter.ac.uk/plagiarism, and www.exeter.ac.uk/mitigation respectively), and that you have read your school's rules for submission of written coursework, for example rules on maximum and minimum number of words. Indicative/first marks are provisional only.

Coursework: I2

Submission Deadline: Thu 28th Apr 2016 12:00

Personal tutor: Professor Gavin Tabor

Marker name: G Tabor

620002200

Word count: 9566



I2 Report

Wind Farm Modelling

Ben Ashby

2015
4th year MEng Group Project

I certify that all material in this thesis that is not my own work has been identified and that no material has been included for which a degree has previously been conferred on me.

Signed..........Ben Ashby.....

I2 Report

ECMM102

Title: Wind Farm Modelling

Word count: 9566

Number of pages: 39

Date of submission: Wednesday, 27 April 2016

Student Name: Ben Ashby

Programme: MEng Mechanical Engineering

Student number: 620002200

Candidate number: 012184

Supervisor: Professor Gavin Tabor

Abstract

This report contributes to the *Wind Farm Modelling* MEng group project, and details the methodology, results, and conclusions of two of the work packages identified within the scope of the wider project. The group project sought to investigate means for the improvement of current modelling practice for wind farms through the evaluation of current techniques and the development of new approaches. The work covered in this report fell into the latter category.

Firstly, a modified version of an existing ‘actuator disk’ turbine model was implemented that actively responds to changes in the incident flow conditions through the use of an upstream velocity sampling patch. The motivation behind these modifications was to allow for better representation of the effects of wake shadowing when modelling large arrays of wind turbines, giving better prediction of power output. This solver was successfully tested, though currently it is highly computationally expensive and so further streamlining may be required before it is commercially useful.

Secondly, a methods based investigation into the use of large experimental datasets for the validation of CFD simulations was undertaken. This work sought to identify statistical and graphical approaches suitable for use validating wind farm models against datasets produced through remote sensing technologies such as LiDAR or SODAR. An experimental dataset generated through Particle Image Velocimetry (PIV) was used for this study, which was compared to CFD simulations run using RANS and LES turbulence modelling. The study found that the RV Coefficient and Sum of Squared Residuals provide a good insight into goodness of fit between large datasets, with the CFD modelling undertaken in this work showing good agreement with the results of the PIV experiment.

Keywords:

Wind Farm Modelling, Actuator Disk, Particle Image Velocimetry (PIV), Model Validation, Large Eddy Simulation (LES), OpenFOAM

Table of contents

1.	Introduction and background.....	1
1.1.	Project Objectives and Deliverables	2
1.2.	Structure of Report.....	2
2.	Literature review.....	3
2.1.	Overview of Subject Area.....	3
2.2.	Wind Turbine Modelling.....	4
2.3.	Validation of CFD Modelling using Experimental Data	4
2.4.	CFD Best Practice for LES Modelling in OpenFOAM	6
2.5.	Data Comparison Techniques for Large Data Sets	6
3.	Theoretical background and Methodology.....	7
3.1.	Actuator Disk Modelling.....	7
3.1.1.	Set up of Model for the SWT-2.3-93 Turbine	7
3.1.2.	Modification of solver to allow for dynamic loading.....	9
3.2.	CFD validation using PIV Datasets	11
3.2.1.	Generation of Experimental Dataset.....	11
3.2.2.	CFD Case Set-Up	12
3.2.3.	Data Comparison Techniques.....	15
4.	Presentation of results.....	17
4.1.	Turbine Modelling.....	17
4.1.1.	Modelling the SWT-2.3-93 Turbine.....	17
4.1.2.	Modified Actuator Disk Solver	18
4.2.	PIV CFD Validation and Data Comparison Methods.....	19
5.	Discussion and conclusions	29
5.1.	Turbine Modelling.....	30
5.2.	Experimental Validation of CFD	30

5.3. Further Work	31
6. Project management, consideration of sustainability and health and safety	32
6.1. Project Management.....	32
6.2. Management of Risks to Project Success.....	32
6.3. Sustainability.....	34
6.4. Health and Safety	34
7. Contribution to group function.....	34
7.1. General Contributions	34
7.2. Actuator Modelling of Wind Turbines in OpenFOAM	35
7.3. Upstream Sampling to set Turbine Characteristics	35
References.....	36

1. Introduction and background

The work detailed in this report contributes to the *Wind Farm Modelling* MEng group project at the University of Exeter. This project seeks to identify means for the improvement of current modelling practice in the design of commercial wind farms through the evaluation and further development of various modelling approaches. This addresses the need to increase the economic viability of wind power, reducing the Levelised Cost of Energy (LCOE) – cost per unit of power generated by a source of energy over its working lifetime – making it more cost competitive with more traditional energy sources (MacKay, 2008). This work was carried out in conjunction with the Centre for Modelling and Simulation (CFMS), a not-for-profit computational modelling research centre, as part of the wider SWEPT 2 research collaboration between a number of research centres and industry specialists in the UK.

The *Wind Farm Modelling* project has been undertaken by a team of 9 MEng students at the University of Exeter. The focus of the work has been split into two main categories: the evaluation of current modelling techniques used to represent wind farms, and the development and implementation of new approaches that offer improved functionality. The work detailed in this report falls into the latter category, with two aspects to the development of improved wind farm modelling being investigated. Initially the focus of this work was on the use of Actuator Disk modelling to model flow at the Rødsand II wind farm in Denmark. As a part of this work, a modified Actuator Disk solver was implemented which actively responds to changing inflow conditions through the use of upstream sampling. This allows for better wake modelling as wake shadowing is included in the setup of individual turbines in an array. It was then hoped to validate these results against LiDAR data for the site. However this data was not made available for use in this work, and so the project brief shifted, using an alternative dataset to investigate methods for CFD validation using large experimental datasets. This investigation was carried out using the results of a Particle Image Velocimetry (PIV) experiment carried out at the University, and aimed to identify methods suitable for use in further work validating wind farm models against data for real world wind farms such as Rødsand II.

This report details the findings of this individual project, for information on the findings of the wider *Wind Farm Modelling* group please see the associated G2 Group Report.

1.1. Project Objectives and Deliverables

As the group project evolved in line with initial findings and external influences (such as the unavailability of the LiDAR data) two work packages were identified to be covered in this individual project. **Table 1** shows each of these work packages along with their associated objectives and deliverables.

The first of these work packages was the modification of an Actuator Disk (AD) model to actively respond to received flow velocity through the use of an upstream sampling patch. Since this model calibrates individual turbines according to the received velocity, rather than the inlet velocity, wake shadowing effects are better represented when modelling large turbine arrays. Once implemented and validated, this approach can be applied to other turbine models, such as the OpenFOAM turbine modelling toolkit developed as a part of the group project.

The second work package was an investigation into the use of large experimental datasets for the validation of CFD results. Since the LiDAR data was not available for use in this project, the alternative PIV dataset was used to develop techniques that could be applied to the validation of turbine modelling with LiDAR or SODAR data in future work.

Table 1: Objectives and deliverables for the work packages addressed in this project

Title	Development of CFD turbine model to respond to variation in flow velocity.	Methods for comparison of CFD results and large experimental datasets.
Objectives	<ul style="list-style-type: none">• Modify AD model to set characteristics according to local wind velocity• Set solver to match power curve of the Siemens SW-2.3-93 wind turbine• Enable better modelling of arrays by setting each turbine according to flow speed at each point in array	<ul style="list-style-type: none">• Recreate results of a PIV experiment investigating wake behind a submerged hull using CFD• Identify methods for the comparison of large datasets which can be transferred to future work comparing wind farm models with site data
Deliverables	<ul style="list-style-type: none">• Implement patch to sample speed upstream of turbine• Modify solver to update thrust and torque for the next time-step according to sampled velocity• Compile and test modified solver	<ul style="list-style-type: none">• Accurate CFD model of case using LES modelling• Validated collection of statistical and graphical data comparison methods

1.2. Structure of Report

This report begins with a review of the literature relevant to the project, before being followed by a description of the theory and methodology used in this work. This is followed by a presentation of the results of this project, leading into a section discussing the results and conclusions of this research. Finally, the project management techniques used throughout the project and the individual contribution made to the overall group project are detailed.

2. Literature review

The following section contains a review of the relevant literature for this project. Initially, the current state of the wind energy industry in the UK is discussed, and research priorities detailed, in order to set this work in context. A discussion of the modelling approaches taken in the literature to investigate the flow behaviour around wind turbines follows this, including a description of the actuator disk model used as a basis for the modified solver implemented in this work.

Following a review of the literature relating to the turbine modelling aspects of this project, relevant studies to the CFD validation investigation are highlighted and discussed. This begins with a discussion of the PIV measurement techniques, including the pros and cons of the approach and a summary of previous work. This is followed by a review of the literature relevant to the setup of the CFD case to be validated. Techniques for the comparison of large data sets, both statistically and graphically are then discussed.

2.1. Overview of Subject Area

Wind energy currently provides the most economically viable alternative to fossil fuels in the UK energy market (MacKay, 2008), and with the UK's large wind resource and increased investment the sector looks to grow in the coming years. As manufacturing efficiency increases and the cost of installation and maintenance falls the economic case for wind energy is set to strengthen (Herp, et al., 2015).

One key area of research is the investigation of the wake region formed behind individual turbines, which is characterised by high wind shear, low energy density, and highly turbulent flow behaviour (Magnusson & Smedmen, 1999). Where turbine wakes coincide with the locations of downstream turbines this causes a reduction in power production, along with increased fatigue of downstream turbines due to increased blade vibration caused by the turbulent airflow (Herp, et al., 2015). This has been identified as a research priority with the view that a better understanding of the influence of turbine wakes can yield a large increase in power production (González-Longatt, et al., 2012). Examples of research in this area in the literature include: (Herp, et al., 2015), (Porté-Agel, et al., 2013), (González-Longatt, et al., 2012).

2.2. Wind Turbine Modelling

In selecting a model for a wind turbine, a compromise between model fidelity and computational expense must be made based upon the scenario in which the model is to be used. Since the aim of this work was model a full wind farm in a single simulation, a computationally inexpensive turbine model was required.

The actuator disk representation of a turbine is commonly used in the literature; considering the volume swept by turbine blades as a disk, across which flow properties are changed to reflect the behaviour of a real turbine (Horlock, 1978). Such models are typically inexpensive and perform well in predicting flow properties in the far wake region (Jeromin, et al., 2013) and so are commonly used in studies concerning large scale modelling and turbine arrays (Castellani, et al., 2013). Simplistic actuator disk models only reproduce linear wake effects, with more complex models including a representation of the rotational effects in the wake (Porté-Agel, et al., 2013), (Svenning, 2010).

More complex models than the actuator disk are available which perform better in the near wake region and better capture more transient flow structures in the wake, such as vortex shedding at blade tips (Kulunk, 2011). However, these models are far more computationally expensive, and so actuator disks are preferred for large scale modelling applications in the literature (Castellani, et al., 2013), (Wu & Porté-Agel, 2013). Accordingly, a variant of the actuator disk model has been selected for use throughout this project (Svenning, 2010). The model includes representation of swirl in the turbine wake through a radial force distribution in the disk based on the Goldstein Optimum (Goldstein, 1929). The performance of this model has been validated for the prediction of wind turbine wake structure against other turbine models (Svenning, 2010), and experimental data from the MEXICO rotor experiments (Jeromin, et al., 2013). The basic Svenning model has been modified for use with multiple turbines to allow for the modelling of arrays (Ashby, 2015), and was used in this work to model the Siemens SWT-2.3-93 wind turbines found at the Rødsand II wind farm in Denmark (4C Offshore, 2012).

2.3. Validation of CFD Modelling using Experimental Data

The over prediction of wind farm power yields by current models is a major motivation for the search for improved modelling techniques (Porté-Agel, et al., 2013). In order to produce better farm models, the performance of models will need to be assessed against the observed flow

distributions at existing wind farm sites. It has been identified by the SWEPT 2 research project (EPSRC, 2015) that further work is required to identify methods for data comparison between the large experimental datasets produced through techniques such as LiDAR and SODAR and the results of CFD simulations.

Notable previous studies in the literature have compared the performance of linear wake models and SODAR data (Barthelmie, et al., 2005), and the results of CFD analysis and LiDAR data for a Wind Farm in complex terrain (Butler & Quail, 2012). However, when it comes to analysing the data both papers have neglected the bulk of the raw data, focussing on subsets for validation purposes, which does not use the data to its full potential. This has meant that there is a real gap in the research, with few studies looking for new methods for validating CFD against large experimental datasets which utilise the full extent of the available data. As a result, the work detailed in this report takes a methods based approach to the comparison of CFD simulations and large experimental datasets, seeking approaches that better utilise the available data. This study was carried out using results gathered through a Particle Image Velocimetry (PIV) experiment carried out at the University of Exeter.

Particle Image Velocimetry (PIV) is a “...non-intrusive laser optical measurement technique for research and diagnostics into flow, turbulence, microfluidics, spray atomization and combustion processes...” (Dantec Dynamics, 2013). The process tracks the motion of particles seeded in the flow to gather highly detailed velocity information for flow in a sample region. Standard PIV measures two velocity components on a plane using a single camera, while Stereo PIV uses two cameras to measure three velocity components on a plane. PIV yields highly accurate datasets and is typically non-intrusive, though in some cases the particles used to seed the flow may not perfectly follow the motion of the carrier fluid (Lignarolo, et al., 2016). Systems often make use of high powered lasers to illuminate the flow field, which brings safety concerns. With the exception of more expensive Stereo PIV systems, PIV neglects the velocity component acting in the z direction (into the camera) and so measurements are limited to 2D planes (Dantec Dynamics, 2013). Previous work validating CFD against PIV data in the literature includes; (Sheng, et al., 1998), (Odemark, et al., 2009), (Lignarolo, et al., 2016). Principle techniques employed in these papers include extracting data to compare plots along lines and visual comparison of contour plots, with little emphasis on comparing the datasets as a whole.

2.4. CFD Best Practice for LES Modelling in OpenFOAM

In order to ensure CFD simulation accurately recreates physical flow behaviour careful setup is required for the meshing, setting of boundary conditions, and turbulence modelling used. When modelling flow in a turbulent boundary layer, the literature recommends a minimum grid spacing of roughly $y^+ = 1$ and dimension ratio within 150:1:40 (x:y:z) to allow for full resolution of flow in the boundary layer (Piomelli & Balaras, 2002). Meshing this high density region can be achieved using the T-Rex application in commercial meshing software Pointwise, producing a high quality boundary layer mesh (Pointwise, 2011).

Sampling data in OpenFOAM can be achieved using the sample utility (CFD Direct, 2015), with options to sample along lines or planes in the domain, and output to files in a number of formats.

2.5. Data Comparison Techniques for Large Data Sets

For the comparison of large datasets there are two main approaches; statistical and graphical (Clark & Ma'ayan, 2011).

One common statistical approach is to analyse the correlation between data sets, for multivariate data this can be done using the RV Coefficient (Robert & Escoufier, 1976). The RV Coefficient is a generalised version of the Pearson correlation coefficient (Josse, et al., 2008), and is calculated according to the variance and covariance between datasets giving values between 0, no correlation, and 1, perfect correlation (Abdi, 2007).

A statistical metric for the closeness of two datasets commonly used in Regression Analysis is the Sum of Squared Residuals (SSR) (Lane, 2012). In order to generalise the SRR value to allow for comparison, datasets can first be normalised to ensure the SRR value reflects the similarity between datasets and not the magnitude of the values within the datasets (Clark & Ma'ayan, 2011).

Graphical approaches such as surface plots, quiver plots, and comparison between subsets of data (such as plotting variation along a line, or across a plane) can be achieved using Matlab, and are all commonly used in the literature: (Barthelmie, et al., 2005), (Butler & Quail, 2012), (Lignarolo, et al., 2016).

3. Theoretical background and Methodology

This section details the methods used throughout this project to achieve the goals set for each work package. Firstly the actuator disk modelling carried out as part of this work is detailed, including a description of the modifications made to the solver. This is followed by a description of the approach taken for the validation of CFD modelling using large experimental datasets.

3.1. *Actuator Disk Modelling*

3.1.1. Set up of Model for the SWT-2.3-93 Turbine

Actuator Disk Model

The wind turbine model used in work is based upon the Actuator Disk model variant implemented in OpenFOAM by Erik Svenning (2010), which has been modified to allow for simulations involving multiple turbines (Ashby, 2015). This model is computationally inexpensive while showing good performance in the prediction of far wake behaviour for wind turbines (Jeromin, et al., 2013).

The user defines the location in mesh, size, thrust, and torque for each turbine and the model distributes these forces across the disk volume according to the Goldstein optimum force distribution (Goldstein, 1929). The power abstracted from the flow by such a model can be found through applying the Conservation of Linear Momentum through a control volume around the turbine (Ashby, 2015).

For a detailed description of actuator disk theory please see (Horlock, 1978), and for more on the Svenning model please see (Svenning, 2010).

Characteristics of Wind Turbine to be modelled

As mentioned previously, an original aim of this project was to produce a CFD model of airflow around the Rødsand II wind farm in Denmark that could be validated against LiDAR data for the site. To this end the actuator disk model was calibrated to recreate the characteristics of the turbine model used on this wind farm; the 2.3MW rated Siemens SWT-2.3-93 (4C Offshore, 2012).

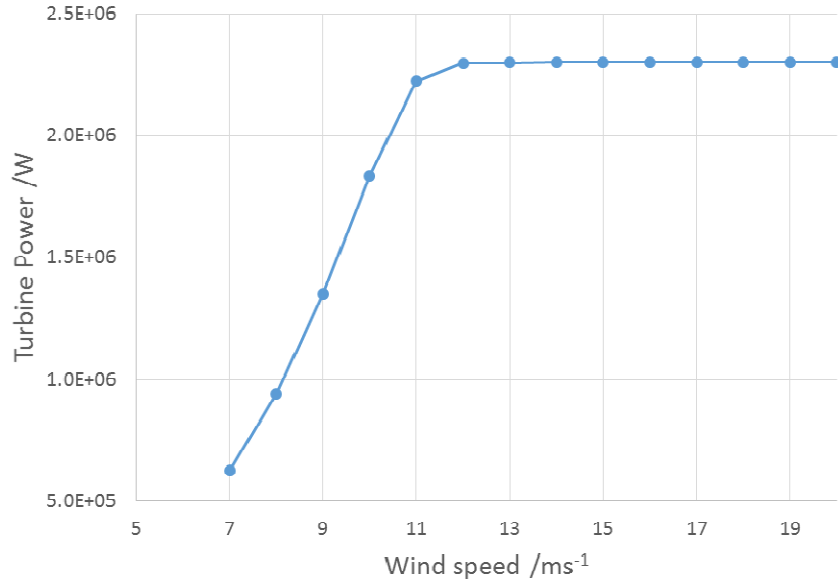


Figure 1: Nominal power curve for Siemens SWT-2.3-93 turbine (4C Offshore, 2012)

This turbine has a rotor diameter of 93m, and is designed for operation in wind speeds of 13.5ms⁻¹. The power curve for this turbine is shown in **Figure 1**.

Calibration of CFD to match turbine characteristics

To recreate the behaviour of the SWT-2.3-93 turbine in OpenFOAM an actuator disk was set up to match the turbine geometry in the domain shown in **Figure 2**.

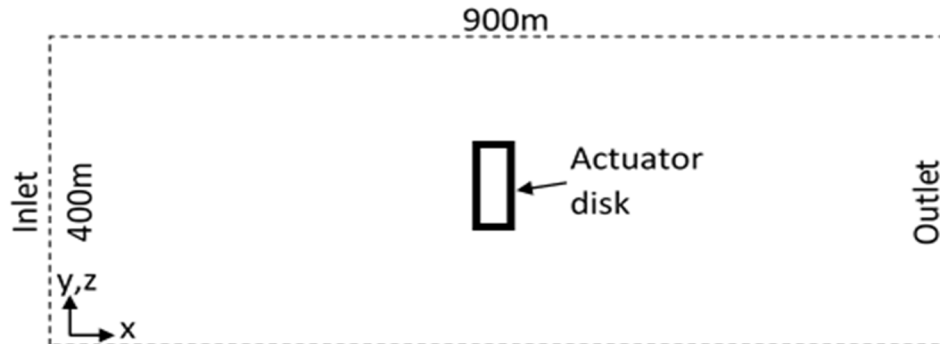


Figure 2: Layout of domain used for turbine calibration

This calibration study aimed to find the required thrust and torque for the actuator disk to recreate turbine behaviour for input flow velocities between 7ms⁻¹ and 20ms⁻¹. The thrust (T) and torque (τ) values for the actuator disk model are set using **Equations 1** and **2**.

Equation 1

$$T = \frac{\rho U_0^2 C_T A}{2}$$

Where: ρ is the fluid density, U_0 is the free-stream velocity, C_T is the thrust coefficient of the turbine, and A is the swept area of the turbine.

Equation 2

$$\tau = \frac{P}{\omega}$$

Where: P is the power abstracted from the flow, and ω is the blade's angular velocity.

For each flow velocity torque was calculated directly from the theoretical power, and a range of possible thrust values was generated through varying values of C_T . Cases were set up with thrust values corresponding to each of these values of C_T . Once run, power abstracted by the actuator disk was found for each case, with the closest to the rated power kept. This built up a close fit to the power curve which can be seen in the results section of this report.

3.1.2. Modification of solver to allow for dynamic loading

Wake shadowing effects in arrays of turbines mean that individual turbines seldom receive clean airflow. The actuator disk model used in this work (Svenning, 2010) requires that turbine thrust and torque are set according to flow velocity, with the free stream velocity therefore being used to assign the thrust and torque for all members of an array. In an effort to more accurately simulate the power production of an array of turbines, a modified solver was implemented to set the turbine thrust and torque according to the incident flow velocity for individual turbines in an array.

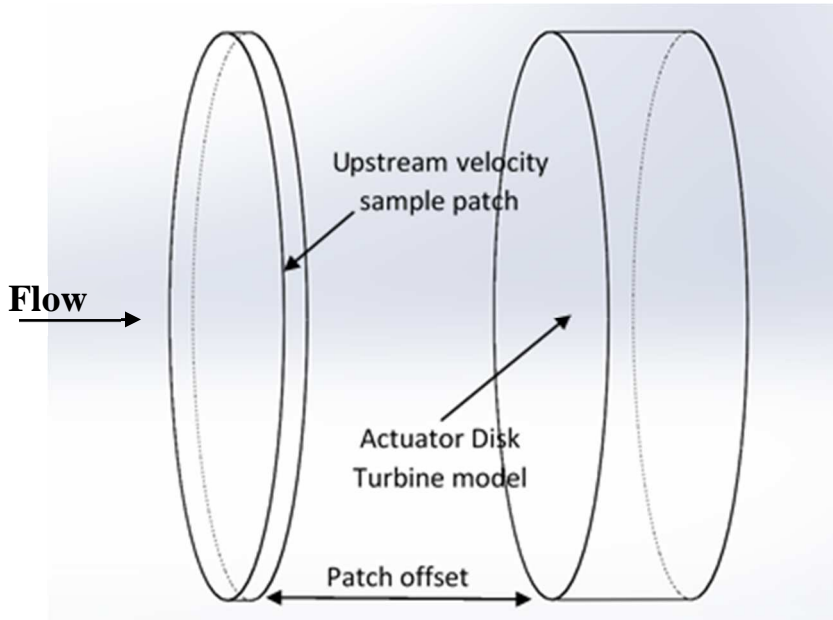


Figure 3: Illustrating the location of the velocity sampling patch in relation to the actuator disk

In order to find the velocity received by a turbine, a sampling patch was used upstream of the turbine as shown in **Figure 3**. The mean velocity of the flow in this patch is found by the solver, and used to select appropriate values for thrust and torque from a look-up table to match the performance of a real turbine.

The main modifications that were made to the solver were implemented in the class descriptor file for the actuator disk objects created by the solver (*'actuatorDiskExplicitForce.C'*). By modifying the class file it was ensured that all turbine objects created for a case inherit the modified attributes. Further modifications were also introduced to the '*turbineProperties*' dictionary which is used to assign the parameters needed to initialise an actuator disk object. This dictionary assigns the parameters needed to describe disk geometry, total thrust, total torque and the density of fluid. Three additional turbine parameters were added to the dictionary:

- *velocityPatchSpacing* enables the user to assign the offset between the sampling patch and the actuator disk
- *velocityPatchThickness* assigns the thickness of the patch enabling the patch to be adapted for use with meshes of various levels of refinement
- *calcStartTime* assigns the time-step at which the thrust and torque values for the turbine switch from the initial values to those calculated from the sampled velocity

To create the upstream sampling patch, a new function was added to the '*actuatorDiskExplicitForce.C*' file called '*'PointIsInSampleRegion'*', which defined the sample region using disk radius, patch thickness, and patch offset. This returns a set of cells which make up the sample patch, across which the averaged velocity was found. The velocity value returned by this function was used to find corresponding thrust and torque values using a look-up table containing the power curve data for the SWT-2.3-93 turbine, with linear interpolation being used to find values for non-integer velocities.

Once the new functions and variables were referenced in the other solver files, the modified solver was compiled and a simple test case designed to assess the solver's functionality. This case used the domain used for the turbine calibration study (**Figure 2**), with an inlet velocity of 13ms^{-1} . The initial values of thrust and torque were set for an inlet velocity of 18ms^{-1} , with the solver switching to calculated thrust and torque values halfway through the simulation. For a correctly functioning solver the expected result for this case would be a clear step up in the thrust value for the turbine after 1000 time-steps (the value of *calcStartTime* used in this case).

3.2. CFD validation using PIV Datasets

3.2.1. Generation of Experimental Dataset

Introduction to PIV

Particle Image Velocimetry (PIV) captures high resolution, instantaneous, velocity data for a flow field through the use of tracer particles seeded in the flow. A laser is used to illuminate the flow in a sample region which is then photographed using a high speed digital camera. Flow velocities for the tracer particles are found from two images taken in quick succession using cross-correlation analysis (Dantec Dynamics, 2013). The sample region is then divided into a grid, with the motion of all particles within each square averaged to give velocity information, producing datasets detailing the velocity distribution across the sample domain. PIV measurements can be taken at very short time intervals to capture transient flow properties with a high level of accuracy. For example, the PIV experiment detailed in this report sampled the velocity in the sample region at 0.067s intervals.

Experimental Setup

The PIV dataset used for the CFD validation study consisted of an investigation into the near wake region formed behind a prismatic hull (see **Figure 4**). The experiment was conducted in the small tilting flume in the University of Exeter's Fluid Dynamics Laboratory under steady state flow conditions. During the experiment, 200 PIV images were taken over 13.267s across a rectangular plane located in the near wake region behind the hull. The raw PIV data was processed using software designed by the manufacturer, Dantec Dynamics, outputting the velocity data into comma separated files containing location and velocity data for each point on the sample grid.

More information on the geometry of the domain used and the flow properties for this experiment are covered in the following section, detailing the process followed to reproduce this experiment in OpenFOAM.

Due to safety concerns associated with the use of a class 4 laser in the PIV equipment, undergraduate students were not permitted to perform this experiment, which was conducted by trained lab technicians.

3.2.2. CFD Case Set-Up

Domain Geometry

Care was taken to ensure that the domain included sufficient upstream and downstream spacing from the hull to minimise the effects of any discontinuities in the flow around the inlet and outlet. To this end one hull length (0.4m) was included between the inlet and the leading edge, and four hull lengths were included downstream of the object. Ideally, this spacing would be larger but due to the computational resources available and time constraints a compromise was made. The domain was set to a depth of 0.131m to match the recorded water depth at the leading edge of the hull.



Figure 4: Layout of domain used to recreate PIV experiment in OpenFOAM

The free surface was represented using a slip boundary condition, while the other surfaces were treated as walls and modelled using appropriate wall functions for each type of turbulence modelling used.

Flow Properties

The mean flow velocity in the flume was found from timed collection data which recorded the mass of water to flow through the flume in a recorded time interval. From this data the averaged mass flow rate for the flume was found, allowing the calculation of the volumetric flow rate and mean flow velocity through the use of simple fluid dynamics principles. This approach gave a velocity value of 0.2263ms^{-1} which was used to set the inlet velocity for the CFD simulations.

From this velocity the Reynolds number was found using **Equation 3**, using the hull length (0.4m) as the characteristic length.

Equation 3

$$R_e = \frac{\rho U l}{\mu} = \frac{998.2 \times 0.2263 \times 0.4}{1.002 \times 10^{-3}} = 90177$$

Where: ρ is the fluid density, U is the flow velocity, l is the characteristic length scale, and μ is the dynamic viscosity of the fluid.

This Reynolds number shows that the flow behaviour around the hull will be turbulent in nature, and so care must be taken in the CFD set-up to select appropriate turbulence modelling and recreate the turbulent boundary layer around the hull to ensure valid results.

In order to accurately reproduce the turbulent boundary layer at the surface of the hull, the mesh was designed to contain a refined region encompassing the boundary layer. The boundary layer thickness was estimated using **Equation 4** (Douglas, et al., 2005). For this case the predicted thickness of the turbulent boundary layer is 0.0156m.

Equation 4

$$\delta = \frac{0.382l}{Re^{0.2}}$$

Where: δ is the boundary layer thickness, l is the characteristic length, and Re is the Reynolds number for the flow.

To accurately recreate the turbulent boundary layer the surface cells were set to a thickness corresponding to $y^+=1$ as recommended in the literature (Piomelli & Balaras, 2002). In this case this corresponded to a grid spacing of 0.0879mm at the wall, calculated using an online mesh design tool (Pointwise, 2016)

Meshing with Pointwise

Once the geometry of the domain to be used had been created in SolidWorks, the domain was imported into Pointwise to begin the meshing process. In order to minimise the computational expense of the simulations, the mesh was designed to contain regions of varying cell refinement, with the highest cell concentrations being found in the fully resolved boundary layer mesh and the sample region (see **Figure 5** for the full cross section of the mesh). A coarser mesh was used further from these areas of interest, such as in the far wake region.

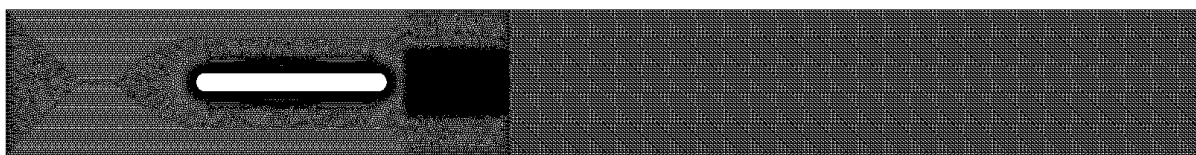


Figure 5: Cross section of meshed domain for the CFD validation study, illustrating the various cell densities used throughout the mesh

The mesh around the sample region is comprised of high density, structured, hexahedra to allow for data to be gathered at a resolution close to the scale of the PIV measurement grid. The mesh surrounding this region and the hull is comprised of unstructured cells, which have been locally refined around the hull in order to fully resolve the turbulent boundary layer.

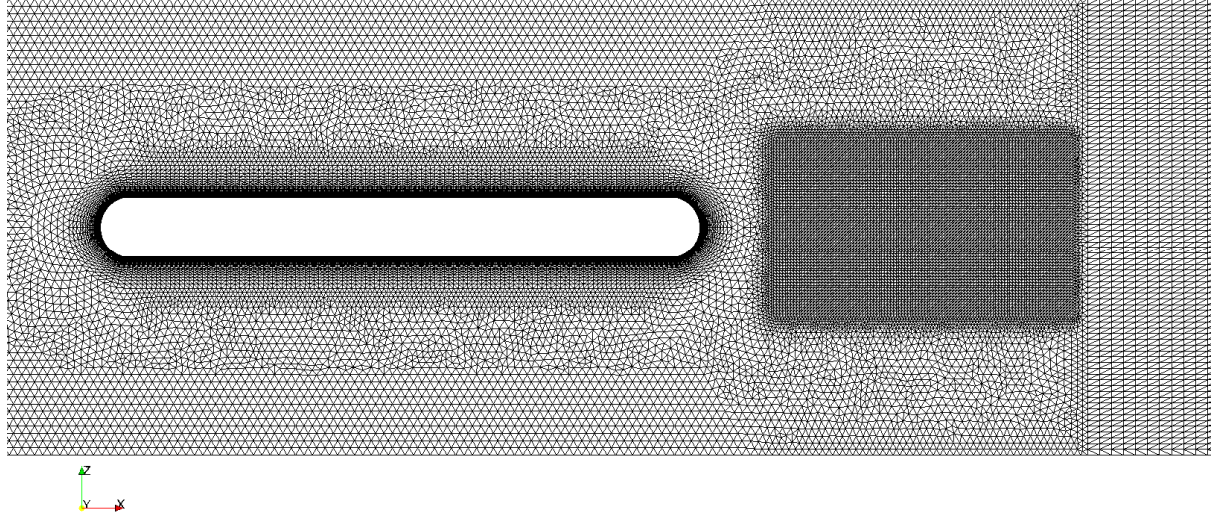


Figure 6: Detailed illustration of varying mesh densities used while meshing the domain

The refined region was introduced into the unstructured mesh using the T-Rex utility in Pointwise, with grid spacing corresponding to a y^+ value of 1, and the dimensions of the refinement zone set according to the predicted boundary layer thickness. The ratio of cell dimensions at the wall was set to 50:1:20 (downstream cell spacing: perpendicular cell spacing: depth cell spacing), well within the guideline of 150:1:40 recommended in the literature (Piomelli & Balaras, 2002). Once the various mesh regions were created, the 2D plane was extruded to produce the full, 3D, domain.

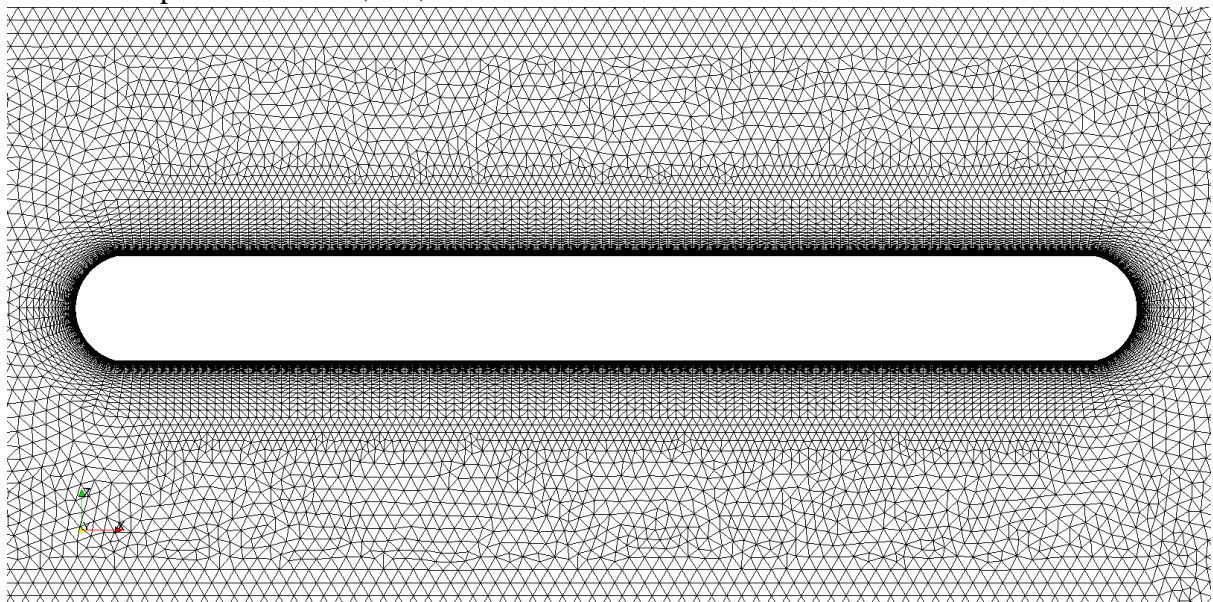


Figure 7: Boundary layer mesh refinement around hull

Turbulence Modelling

Two approaches have been taken to the modelling of turbulence in this work: steady-state RANS modelling was initially used due to its lower computational cost and versatility, before Large Eddy Simulation (LES) was conducted in an effort to reproduce the more complex, time dependent turbulent structures visible in the PIV results.

Since RANS modelling produces a time averaged representation of turbulent behaviour its use for validation against the transient PIV data is limited, impacting the ability to utilise the full data set to its potential. In this project the k-Epsilon model was used as an initial approach to test the case set-up and mesh, and the resulting data used to compared to the time averaged PIV data in order to explore comparison techniques while allowing the more computationally expensive LES simulations to complete.

On concluding the RANS modelling for the domain, the case was modified for use with the pimpleFoam solver using the Smagorinsky LES model.

Sampling

In order to sample velocity data from the CFD simulations, the sample utility in OpenFOAM was used (CFD Direct, 2015). Once set up, this utility outputted the velocity components and magnitude in comma-separated (.csv) format a grid corresponding to the PIV experimental data, ready for analysis and comparison. This sampling approach was run once the simulations had completed, saving the sampled data for each saved time-step present in the case.

3.2.3. Data Comparison Techniques

Processing the Raw Datasets

In order to compare the PIV and CFD datasets each required significant manipulation to achieve compatible formats. Due to the large numbers of PIV datasets a script was written to automate the import process in Matlab, enabling the creation of 200 separate 15914x4 arrays containing location and velocity component data for each time step. The 3rd and 4th columns of this output was comparable to the data gathered by the sample utility. This data was imported into Matlab in the form of 15914x2 matrices containing the velocity component data, ordered to match locations of each data point in the PIV dataset.

The raw PIV data contained some error values, denoted by ‘nan’ (not-a-number) in Matlab which required removal before scripts such as the correlation coefficient calculation, or data normalisation, could be executed. The replacement of such values with zero terms was included into the import script once these errors were identified to ensure all subsequent data processing could be run successfully.

Correlation coefficient

The RV Correlation Coefficient for use with multivariate datasets is given as (MathWorks, 2016):

Equation 5

$$r = \frac{\sum_m \sum_n (A_{mn} - \bar{A})(B_{mn} - \bar{B})}{\sqrt{\left(\sum_m \sum_n (A_{mn} - \bar{A})^2\right)\left(\sum_m \sum_n (B_{mn} - \bar{B})^2\right)}}$$

Where: A and B are two $m \times n$ matrices to be compared.

The correlation coefficient gives values between -1, perfect negative correlation, and 1, perfect positive correlation. For more on the mathematics and implantation of this metric the reader is directed to: (Josse, et al., 2008), (Abdi, 2007) and (MathWorks, 2016).

Sum of Squared Residuals (SSR)

One metric for the closeness of fit often used in areas such as Linear Regression is the Sum of Squared Residuals (SSR) which is given by **Equation 6**:

Equation 6

$$SSR = \sum (\hat{Y} - y)^2$$

Where: \hat{Y} is the value of a point in the experimental dataset, and y is the approximation to the value given by the model.

This metric gives a good indication of the goodness of fit between datasets, and the individual squared residuals can be used to produce error distribution plots, aiding in the identification of areas of poor fit. Unlike the Correlation Coefficient the output of the SSR is not bounded, with the magnitude of the results depending on the data used.

4. Presentation of results

This section details the results achieved throughout this project, beginning with the modified actuator disk solver, followed by the results of the PIV CFD validation work.

4.1. *Turbine Modelling*

4.1.1. *Modelling the SWT-2.3-93 Turbine*

The actuator disk model used to model the SWT-2.3-93 turbine provided a good representation of the wake structure and abstracted power at a relatively low computational cost. For a mesh containing 1,387,336 cells, a simulation run for 5000 time-steps took 5h23m to complete on a PC with a quad core 3.4GHz processor.

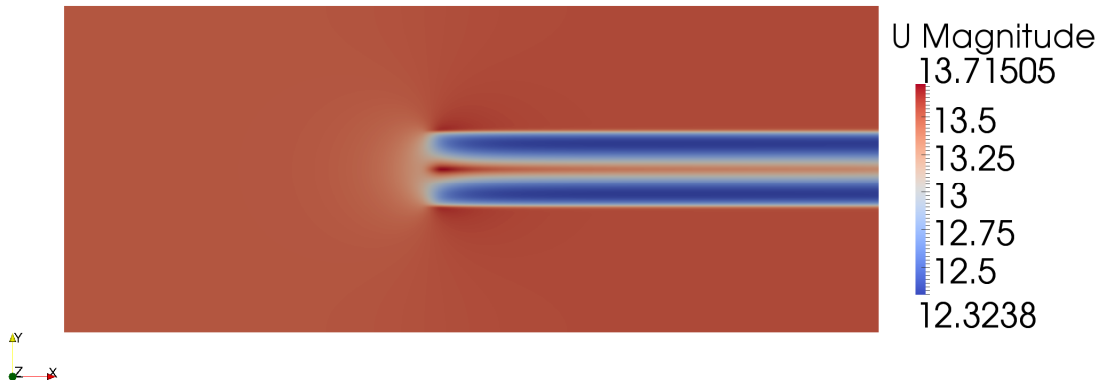


Figure 9: Velocity contours throughout domain, showing wake region formed behind disk

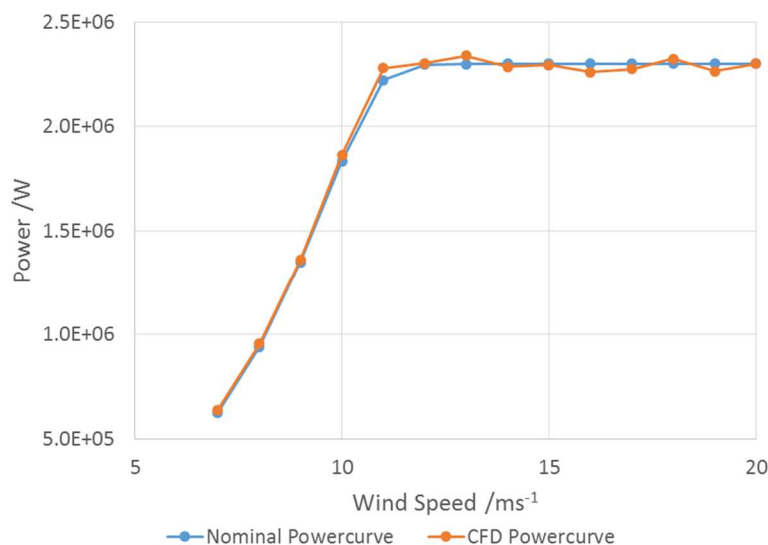


Figure 8: Power curve of actuator model compared to the nominal power curve of the SWT-2.3-93 turbine

Through the investigation of various thrust coefficient values a CFD model for the SWT-2.3-93 turbine was achieved with a power curve as shown in **Figure 8**. This provided a close match to the stated power curve for this turbine which was published online (4C Offshore, 2012).

Once this power curve was recreated in CFD, the thrust and torque values required to give the right power abstraction for the flow velocity could be used in a look-up table to automatically assign thrust and power based on input speed. This look-up table was crucial to the implementation of the modified actuator disk solver.

4.1.2. Modified Actuator Disk Solver

Once the modified actuator disk solver was successfully compiled a simple test case was run, with incorrect thrust and torque values for the flow speed assigned initially and the calculated thrust and torque values implemented after 1000 time-steps. In this case, the thrust and torque values were set using values calculated for a flow speed of 18ms^{-1} , with the real speed used for this case being 13ms^{-1} . This test case was successful in that the thrust and torque values were reset according to the sampled velocity upstream of the disk (see **Figure 10**). However, this modified solver was very computationally expensive compared to the original solver, taking a week to run on the same mesh and machine that ran in 5h23m using the original solver. There is scope for streamlining the solver however, with this initial compilation being relatively crude in its implementation. The success of the upstream sampling approach, which allows turbine models to dynamically respond to their incident flow properties, could lead to more accurate prediction of array power than previous modelling approaches.

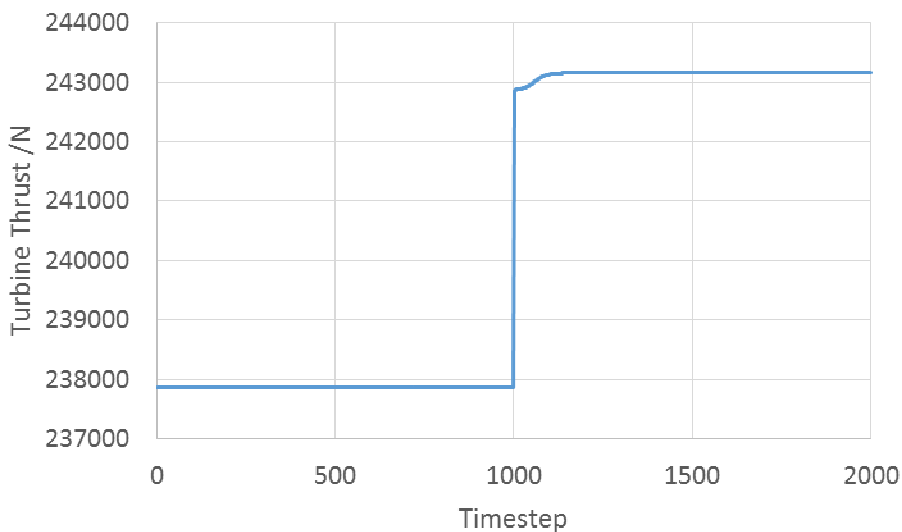


Figure 10: Turbine torque against time-step for the modified solver test case, illustrating the implementation of the active calculation after 1000 time-steps. The calculated value is shown to settle within 150 time-steps of the calculation being implemented for this case.

4.2. PIV CFD Validation and Data Comparison Methods

This section details the results of the CFD simulations, and the techniques used to compare these results with the PIV dataset. Since the RANS simulation completed before the LES simulation, the results were used to establish a number of techniques for data comparison and to lay the foundation for the comparison with the LES simulations.

Results and Comparison for the RANS Simulation

Upon running the case using the K-Epsilon turbulence model, velocity contours as shown in **Figure 11** were achieved for the domain, clearly showing the wake region formed behind the hull.

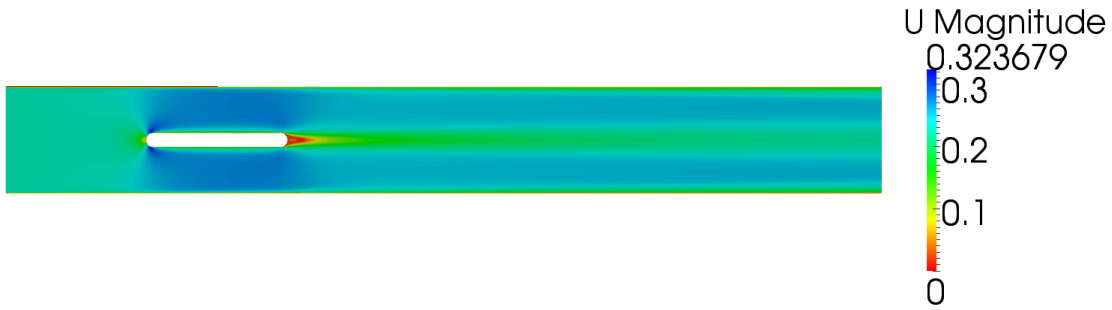


Figure 11: Velocity contours throughout domain for the RANS simulation after 1500 time-steps

Since RANS reproduces the steady state flow behaviour, the case was compared to the averaged PIV data to reduce the discrepancies between the datasets caused by transient flow properties shown in the PIV results. This averaging processes greatly reduces the amount of information available for the comparison, and was only used to develop comparison methods that could later be applied to the transient LES results.

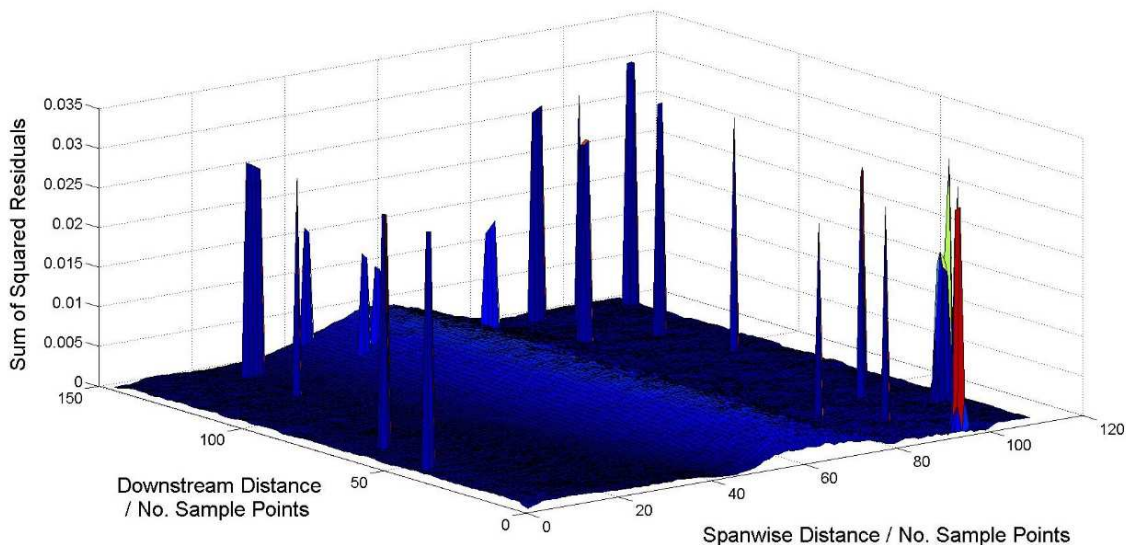


Figure 12: Surface plot of squared residuals between RANS data and time averaged PIV results without removal of anomalies in PIV data

Upon comparison with the raw averaged PIV data, the results of the RANS simulation returned a matrix correlation coefficient of 0.977, showing a close match between the two datasets. The sum of squared residuals (SSR) was 0.13 between the raw datasets. Upon plotting the distribution of this error throughout the sample domain it became apparent that a large proportion of the error could be attributed to anomalies in the PIV results, where small regions of the sample area recorded negligible velocities across all timesteps (see **Figure 12**).

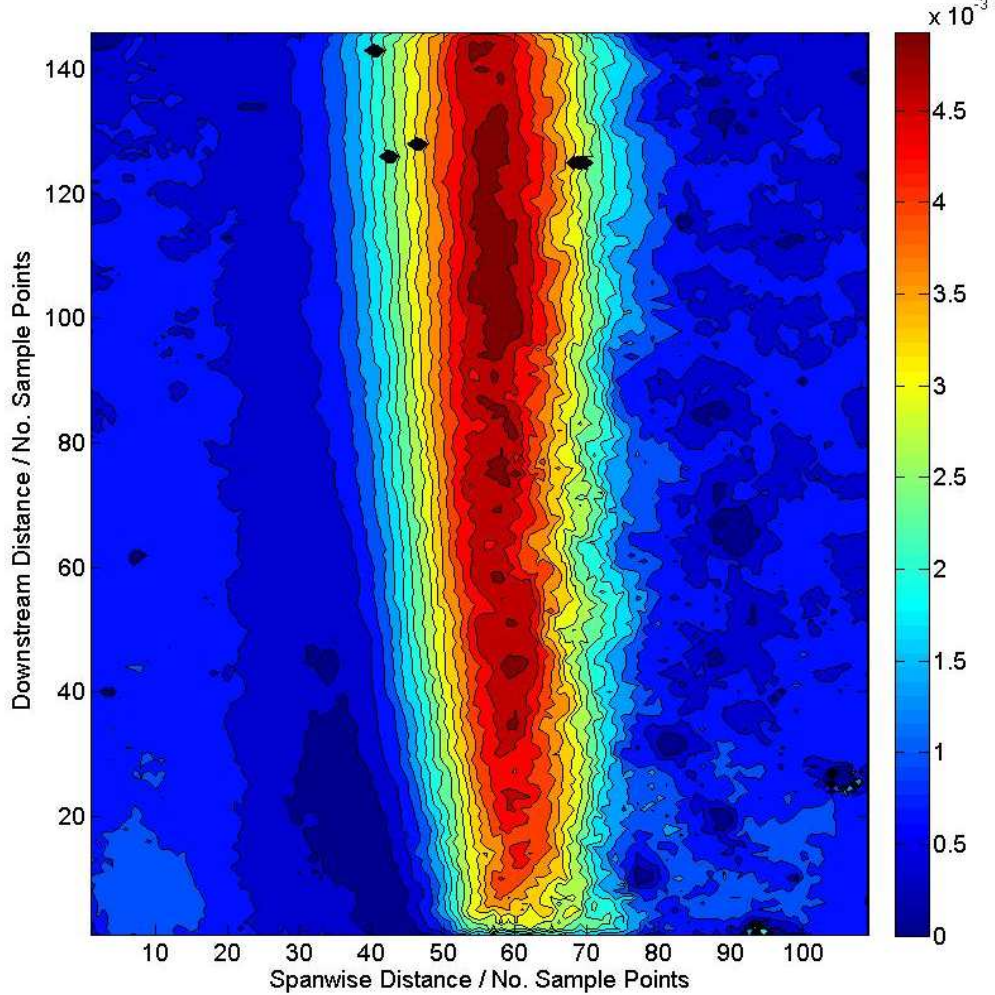


Figure 13: Contour plot of Sum of Squared Residuals between the results of the RANS simulation and the time averaged PIV data once anomalies had been removed

Once the data was filtered, the correlation between the datasets increased to 0.991, and the SRR reduced to 0.052. The error distribution plot between the CFD results and filtered PIV (**Figure 13**) shows the majority of the discrepancies between datasets lies in the wake behind the hull, as would be expected. Though the sample domain is not large enough to show the full wake, the contour plot indicates that the residuals between datasets increase with downstream distance in the wake. In order to assess whether this is due to an underprediction or overprediction of flow velocities in the CFD simulation, velocity magnitude was found for each

dataset and a surface plot of the residuals between the two was produced (see **Figure 14**). The plot shows that the velocities were lower in the CFD simulation throughout the domain. This may be attributed to uncertainties present in the measured mean velocity from the original experiment, which was used to setup the CFD case.

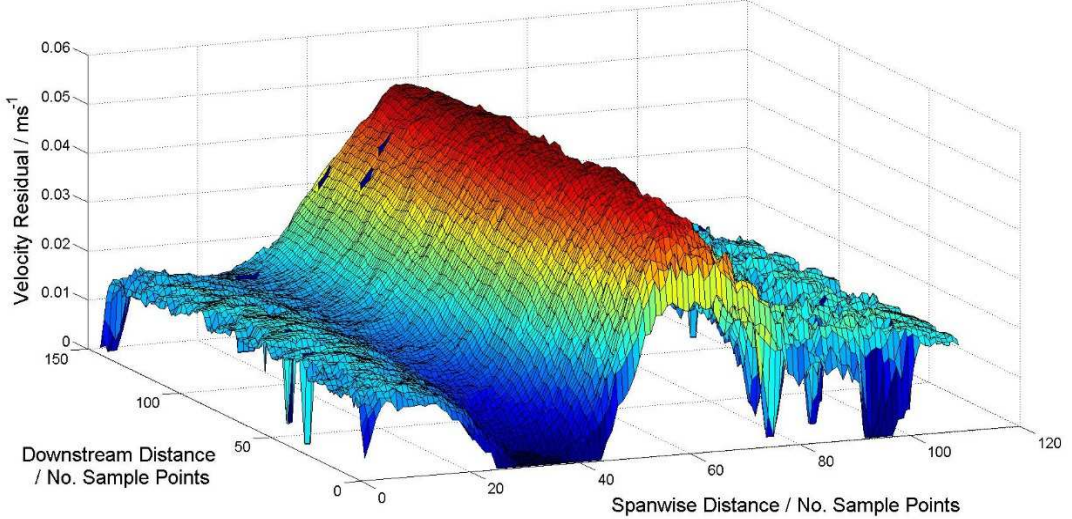


Figure 14: Velocity residuals between the averaged PIV data and RANS data, since the residuals are positive throughout, this shows that RANS under predicted the flow velocities in the sample region

Figure 14 shows increased residuals in the wake region, with residuals also increasing with downstream distance. This suggests that the simulation is under predicting the rate of wake recovery in the sample region.

Results and Comparison for the LES Simulation

Upon running the simulation using Large Eddy Simulation, vortex shedding was apparent in the wake structure with a clear vortex street formed in the region behind the hull. The wake region expands as it moves downstream as the vortices dissipate. **Figure 16** shows the formation of turbulence along the hull, before the turbulent boundary layer detaches at the trailing edge. Vortices form in the low pressure region beyond the boundary layer separation before being shed and dissipating as they move downstream. The progression of vortices in the wake behind the hull is illustrated in **Figure 15**.

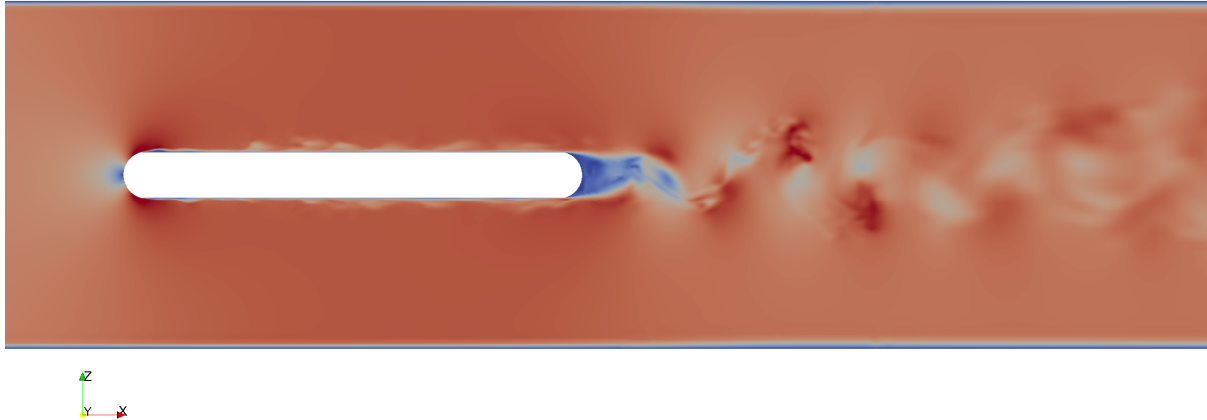


Figure 165: Vortex structure in the near wake region produced by the LES run after 8.5s

The LES simulation for this case was highly computationally expensive due to the highly refined cells in the boundary layer mesh restricting the maximum allowable time-step for stable simulation to around 0.005s. The simulation took 3 weeks and 2 days to complete when run on 2 processors of a machine with 12 processors that run at 3.47GHz, with 50GB of RAM. The case was setup to simulate the flow over a 10 second period, with the mesh containing 7,328,880 cells. A running period of 10 seconds was chosen to allow the flow to propagate through the domain fully.

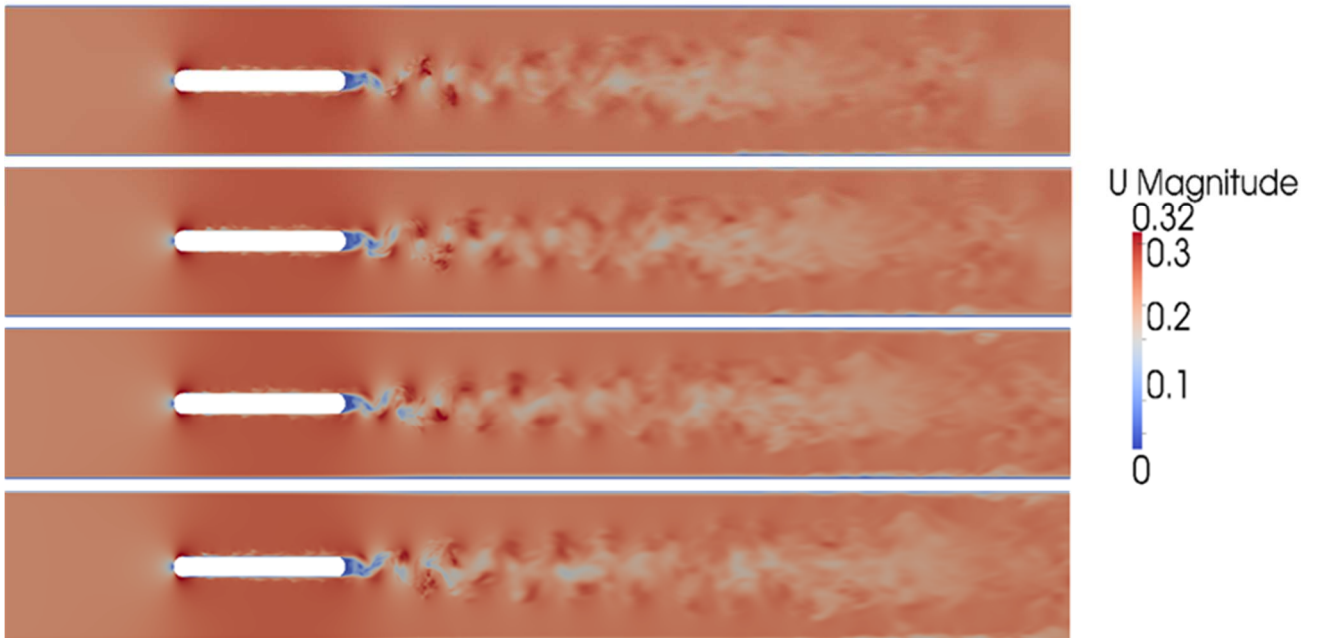


Figure 15: Velocity contours for domain at $t=8.5s, 9s, 9.5s, 10s$ (from top to bottom) for LES simulation

Since both the LES simulation and PIV results captured the transient flow structures there was a lot of variation between data for each time-step. To ensure that the comparison between datasets was valid, with the two datasets being ‘in phase’ with each other, a search function

was written to match datasets according to the SSR. For each CFD dataset imported from the LES results the function loops through the 200 PIV data files, identifying the closest fit based on SSR, whilst also returning the Correlation Coefficient. Plots of error distribution and corresponding velocity magnitude distributions are then plotted automatically, the results of which have been shown for 4 time-steps tested over the following pages.

For the LES simulation at t=8.5

Best fit was the 164th PIV dataset with a SSR score of $0.0023\text{m}^2\text{s}^{-2}$.

The corresponding Correlation Coefficient was 0.9543.

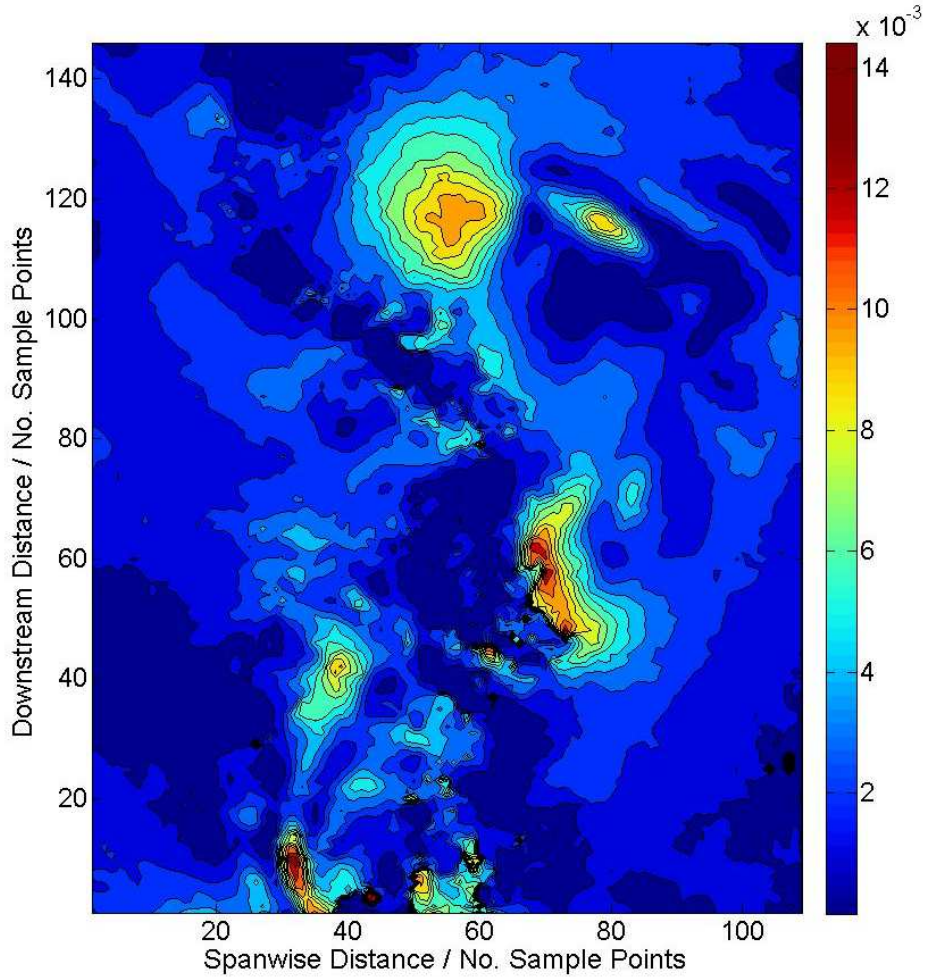


Figure 17: Distribution of the squared residuals of velocity between the LES simulation after 8.5s and the 164th PIV dataset

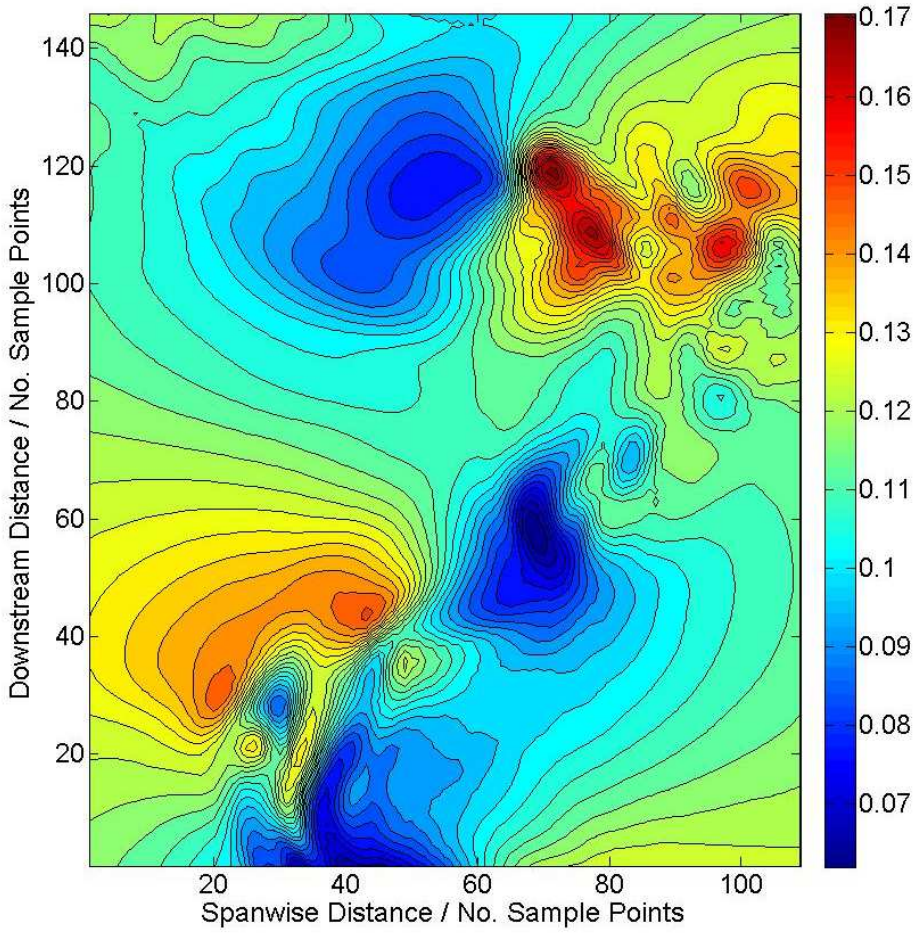


Figure 18: Contours of velocity magnitude for LES simulation at $t=8.5$ s

As with the RANS simulations, the error is concentrated in the areas with the minimum velocity in the wake region, with further analysis revealing the CFD simulations were predicting lower velocities than were observed. Away from the velocity minima there is little error between the experimental results and the simulation.

Despite the error concentration in regions of low velocity, the overall error is low and there is a high degree of correlation between the datasets.

For the LES simulation at $t=9$

Best fit was the 54th PIV dataset with a SSR score of $0.0021\text{m}^2\text{s}^{-2}$.

The corresponding Correlation Coefficient was 0.9497.

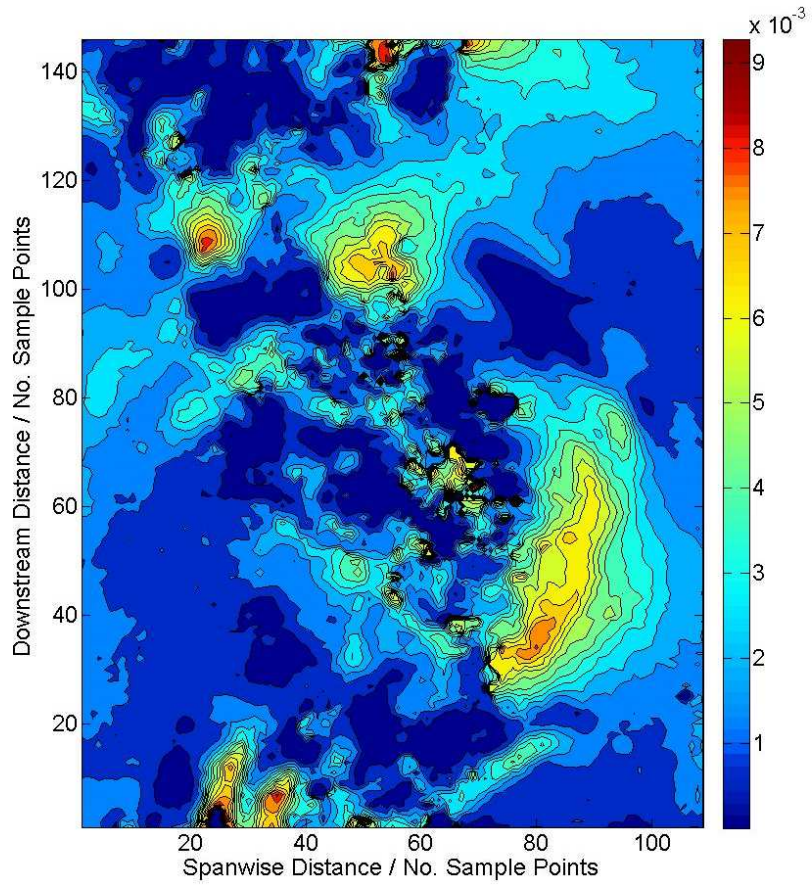


Figure 19: Distribution of the squared residuals of velocity between the LES simulation after 9s and the 54th PIV dataset

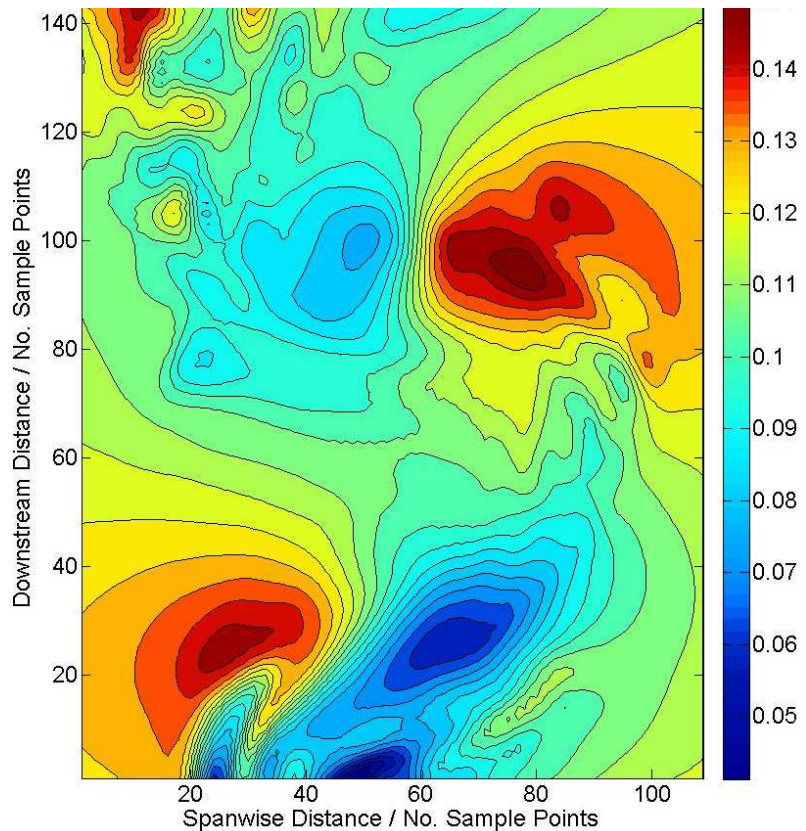


Figure 20: Contours of velocity magnitude for LES simulation at $t=9s$

The error distribution for this time-step does not correspond as closely to the velocity minima as the previous time-step, though there is still an apparent connection between the error concentrations and the low velocity areas. The overall error between these datasets is lower than the previous case and distributed more evenly and there is a strong correlation.

For the LES simulation at t=9.5

Best fit was the 171st PIV dataset with a SSR score of $0.0026\text{m}^2\text{s}^{-2}$.

The corresponding Correlation Coefficient was 0.9163.

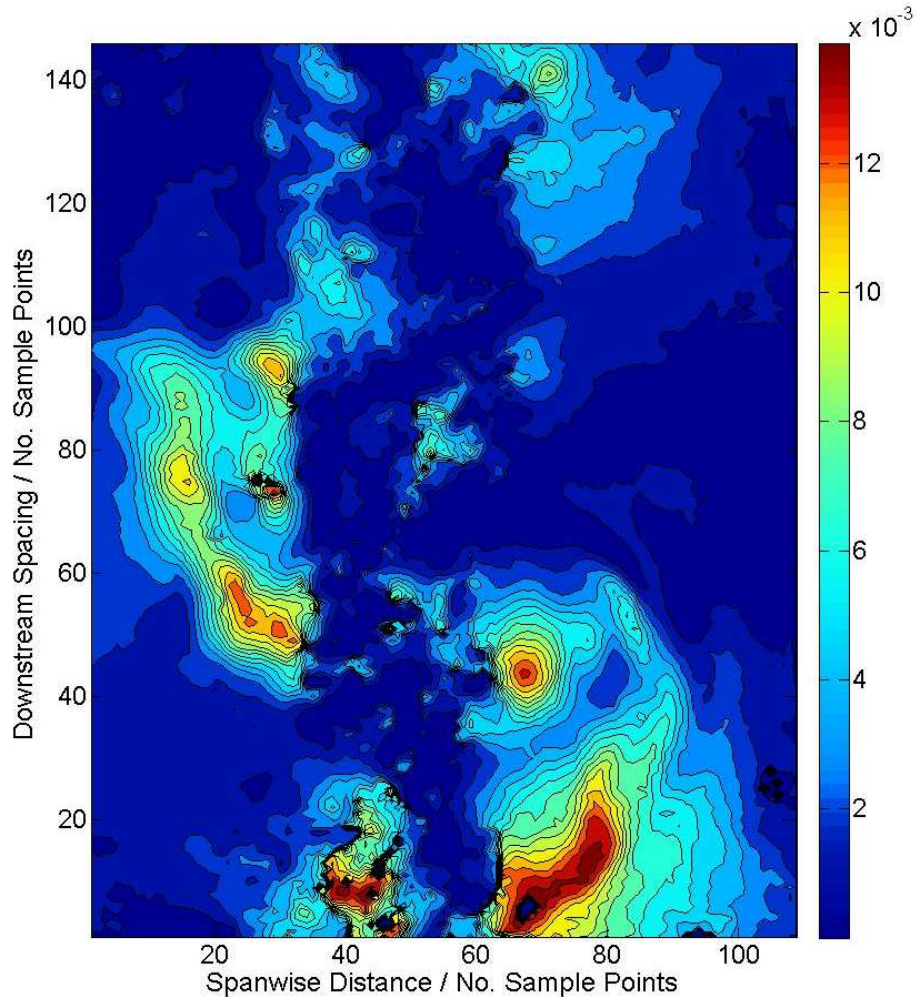


Figure 21: Distribution of the squared residuals of velocity between the LES simulation after 9.5s and the 171st PIV dataset

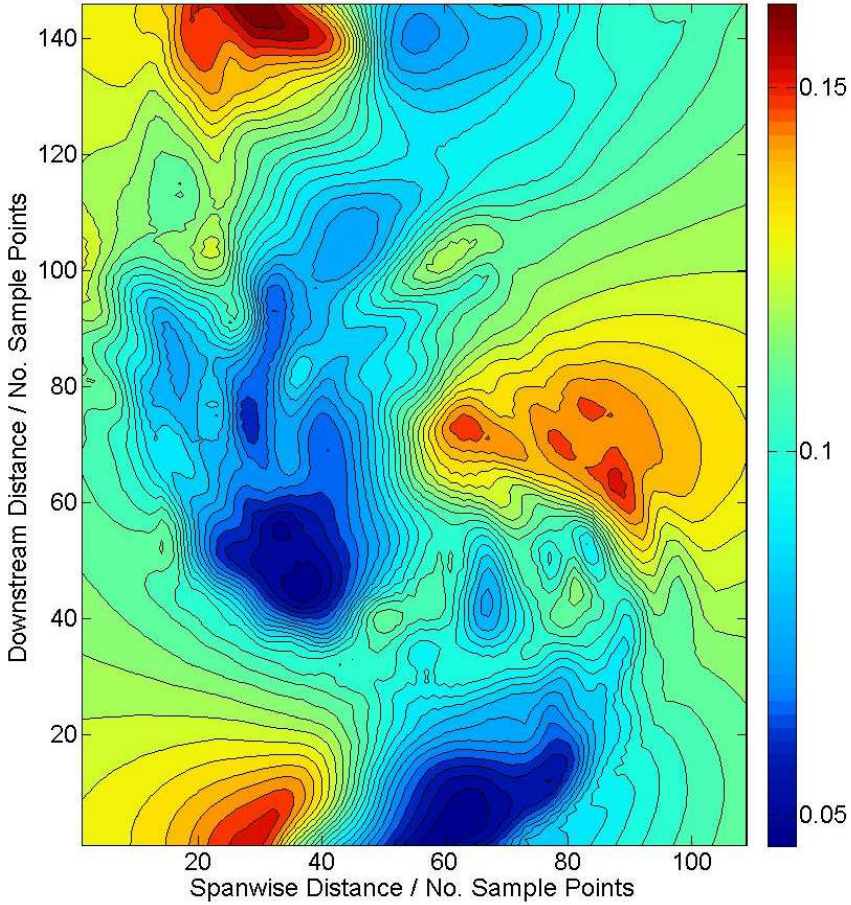


Figure 22: Contours of velocity magnitude for LES simulation at $t=9.5\text{s}$

There is a very strong correspondence between the error concentration and the location of the velocity minima in this case, with the locations of these regions almost exactly matching each other. Away from these regions the error is small, and there is otherwise a high degree of correlation between the datasets. As with the previous cases it was found that the CFD simulation was predicting lower minimum velocities in the wake than was observed by the PIV experiment.

For the LES simulation at $t=10$

Best fit was the 80th PIV dataset with a SSR score of $0.0027\text{m}^2\text{s}^{-2}$.

The Corresponding Correlation Coefficient was 0.8964.

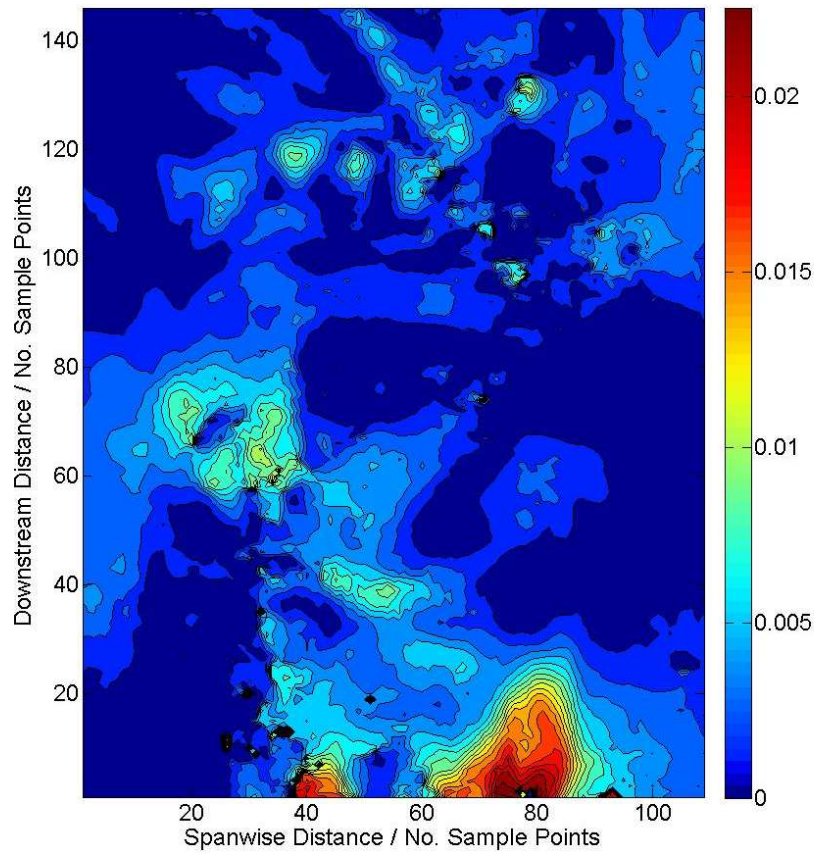


Figure 23: Distribution of the squared residuals of velocity between the LES simulation after 10s and the 80th PIV dataset

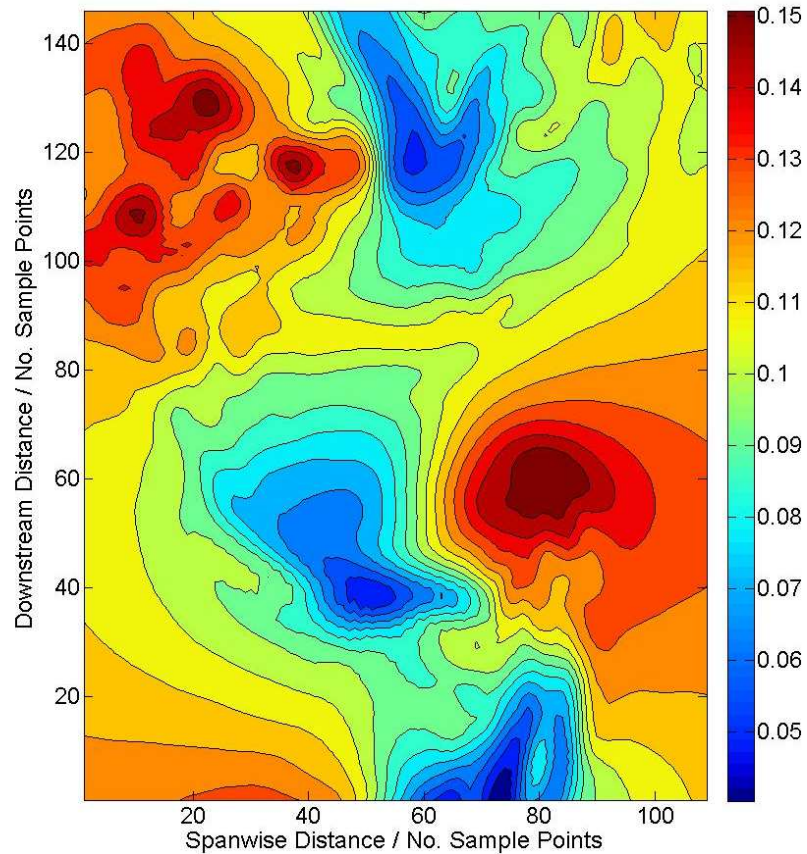


Figure 24: Contours of velocity magnitude for LES simulation at $t=10$ s

This data pairing had the highest SSR of the cases compared, though the majority of this error can be attributed to the low velocity region located at the bottom of the plot where there is a very high error concentration. Away from this region the error is far lower, though it still corresponds to slow moving areas in the wake. The correlation is also lower than for other cases, again this linked to the poor prediction of the wake structure at the bottom of the image.

Summary of Data Comparison Results

The data comparison techniques used in this work allowed for the analysis of the overall error between datasets, and allowed for areas of discrepancy to be easily identified. The goal of the validation in this case was to check that the turbulent wake structures simulated by the CFD were of similar form to the observed wake structure. Due to the random nature of the turbulence in the wake, the fact that the closest fitting PIV datasets to the CFD simulation were not at 0.5 second intervals corresponding to the CFD data is not surprising. The close fit between the observed and predicted structures suggests that the CFD simulation has produced a good representation of the real flow behind the hull.

The techniques used in this work have only addressed the comparison of data on a plane, since the PIV data was limited to two dimensions. The remote sensing technologies used to measure airflow at wind farm sites are capable of producing flow datasets in three dimensions. Techniques such as SSR and other measures of goodness of fit of this type (Root Mean Square Error and others) are still of use in this situation. Graphical approaches and the RV Correlation Coefficient would require the data to be sampled to provide 2D datasets. Since much of the surveying work being carried out using LiDAR produces 2D datasets this should not be a problem, but as more advanced measurement systems become more widely used comparison techniques that can be applied in 3D may require further development.

5. Discussion and conclusions

Overall, this individual project has delivered on both work packages set as part of the wider *Wind Farm Modelling* project. A modified actuator disk solver has been implemented which actively responds to flow velocity through the use of an upstream sampling patch. This paves the way for further development of more accurate array modelling approaches that better predict wind farm power output. In addition to this solver, the validation of CFD modelling against large experimental datasets has identified a number of approaches suitable for use in

the validation of wind farm models. These techniques can be used to compare the results of such models with data gathered at wind farm sites by remote sensing technologies such as LiDAR and SODAR.

These work packages have contributed towards the development aspect of the *Wind Farm Modelling* project, highlighting useful techniques to be used in further work in the area. The following subheadings cover conclusions specific to each work package, before detailing areas of further work based on this reports findings.

5.1. *Turbine Modelling*

The actuator disk model used in this work achieved a close match to the available performance characteristics for the Siemens SWT-2.3-93 wind turbines used at the Rødsand II offshore wind farm. From this model, the solver was modified to actively respond to the incident flow conditions. This modified solver performed as expected for the test case, successfully altering the turbines thrust and torque in response to the inlet velocity, though the implementation of this modification into the solver has caused it to become highly expensive to run.

This modified solver was produced to test the approach and the sampling patch code was introduced rather crudely into the solver class. At each time-step, the solver loops through all cells in the mesh to identify cells that make up the sampling patch. If cells in the patch were identified at the first time-step and this cell set saved for use with all subsequent time-steps the operation of the solver would not be significantly slowed by the sampling patch modification.

This upstream sampling approach has been shown to work in OpenFOAM and if the above modification was made to reduce the computational cost, the modified solver could be used to better predict power production for an array of wind turbines. The code for this modified solver will be made available along with the other resources generated by the *Wind Farm Modelling* project.

5.2. *Experimental Validation of CFD*

The CFD simulations carried out to reproduce the results of the PIV experiment both gave good representations of the flow in the sample region. The RANS simulation provided a good fit to the time averaged PIV data, with a SSR of 0.052 and correlation of 0.991 once anomalies in the experimental dataset were removed. When run using LES, the case produced a turbulent wake structure that was consistent with that observed in the PIV datasets, for the 4 time-steps tested, the average SSR was 0.0024 and the average correlation was 0.929. For both the RANS

and LES simulations, the error between the observed wake structure and the simulation results was concentrated in the regions where the velocity was lowest. Since the accuracy of simulations is tied to the mesh used, increasing mesh resolution could reduce these discrepancies.

For the comparison of CFD with raw experimental data, much manipulation is required to process the data into a comparable form. This manipulation is highly dependent on the format of the raw data, and so this stage in the validation process cannot easily be generalised for all cases. Once the data is of comparable form, this report found that the RV Correlation Coefficient is useful for giving an indication of fit between 2D datasets. Since this metric returns values between 0 and 1, the result can be used to draw an immediate conclusion on fit. It was found that the Sum of Squared Residuals gives a good indication of fit, and the squared residuals can be used to plot error distribution throughout a domain. This approach can be extended for use with 3D datasets. Depending on the format of the experimental data, either one of these approaches can provide useful information on the overall fit of the dataset without the need for subsampling.

5.3. Further Work

The results of the work presented in this report have led to the identification of a number of areas for further work. The outcomes of each work package could be combined and applied to the modelling of the Rødsand II wind farm if the LiDAR data were to be made available. If the modified actuator disk solver was updated to fix the high computational cost of the current implementation it could be used to simulate the flow throughout Rødsand II. Predicted power could be compared to real operating data from the farm, and the data comparison techniques outlined in this report could be used to validate the modelling against the LiDAR dataset. Further work on the development of statistical tests to assess the fit between datasets could also be pursued, with Bayesian statistics offering a potential area of investigation (Gelman, et al., 2013).

Alternatively, as an extension to the creation of the modified actuator disk solver, a more generic implementation of the upstream sampling approach could be developed. If successful this functionality would then be easy to add to a range of other CFD models, and could make up part of the OpenFOAM turbine modelling toolkit developed as part of the *Wind Farm Modelling* project.

6. Project management, consideration of sustainability and health and safety

6.1. Project Management

In order to ensure this individual project successfully delivered on the assigned work packages, producing results that contributed to the aims of the overall group project, it was managed carefully over its duration. Weekly meetings with the other group members and the project supervisor Professor Gavin Tabor, served as a platform to discuss progress, helping to guide each individual towards a set of meaningful outcomes within the overall scope.

Throughout the course of the individual project a Gantt chart (**Figure 25**) was used to aid time management. As the nature of the research evolved in response to both initial findings and external pressures this Gantt chart was updated, ensuring the project was always guided by a set of structured targets.

6.2. Management of Risks to Project Success

Throughout this work an effort was made to anticipate any threats to project success in advance, and plan for the mitigation of any adverse effects these threats may carry. **Table 2** shows the risk assessment table included in the initial project report. It was identified early on in the project that the LiDAR data for the Rødsand II wind farm may not be available in time for use in this work. Accordingly, the PIV experimental dataset was identified as an alternative, ensuring that the proposed investigation into data comparison techniques could still take place.

Table 2: Risk Assessment from I1 report, showing perceived risks to project success at the half way mark (Ashby, 2015)

ID	Risk Item	Effect	Cause	Likelihood	Severity	Importanc	Action to minimise risk
1	Loss of Work	Wasted time as work is re-done	-Not backing up work -IT issues	2	6	12	-back up all work on external hard drive and OneDrive
2	Delays in Accessing LiDAR data	Time delays causing project deadlines to be missed	-Protocols for the release of data -Delays from project partners	5	9	45	-Make sure contingency plans are in place if data is unavailable -Identify need for data ahead of time to allow for delays
3	Project delays due to other commitments	Project falls behind schedule	-lack of planning	2	4	8	-Plan project work around other commitments in advance -Concentrate work at times where there are no other commitments
4	Modelling issues	Delays as tasks take longer than predicted	-lack of proper planning -unforeseen issues/technical challenges	6	4	24	-Allow plenty of time for tasks -Include some flexibility in time management plans to allow for issues and minor delays

Gantt Chart

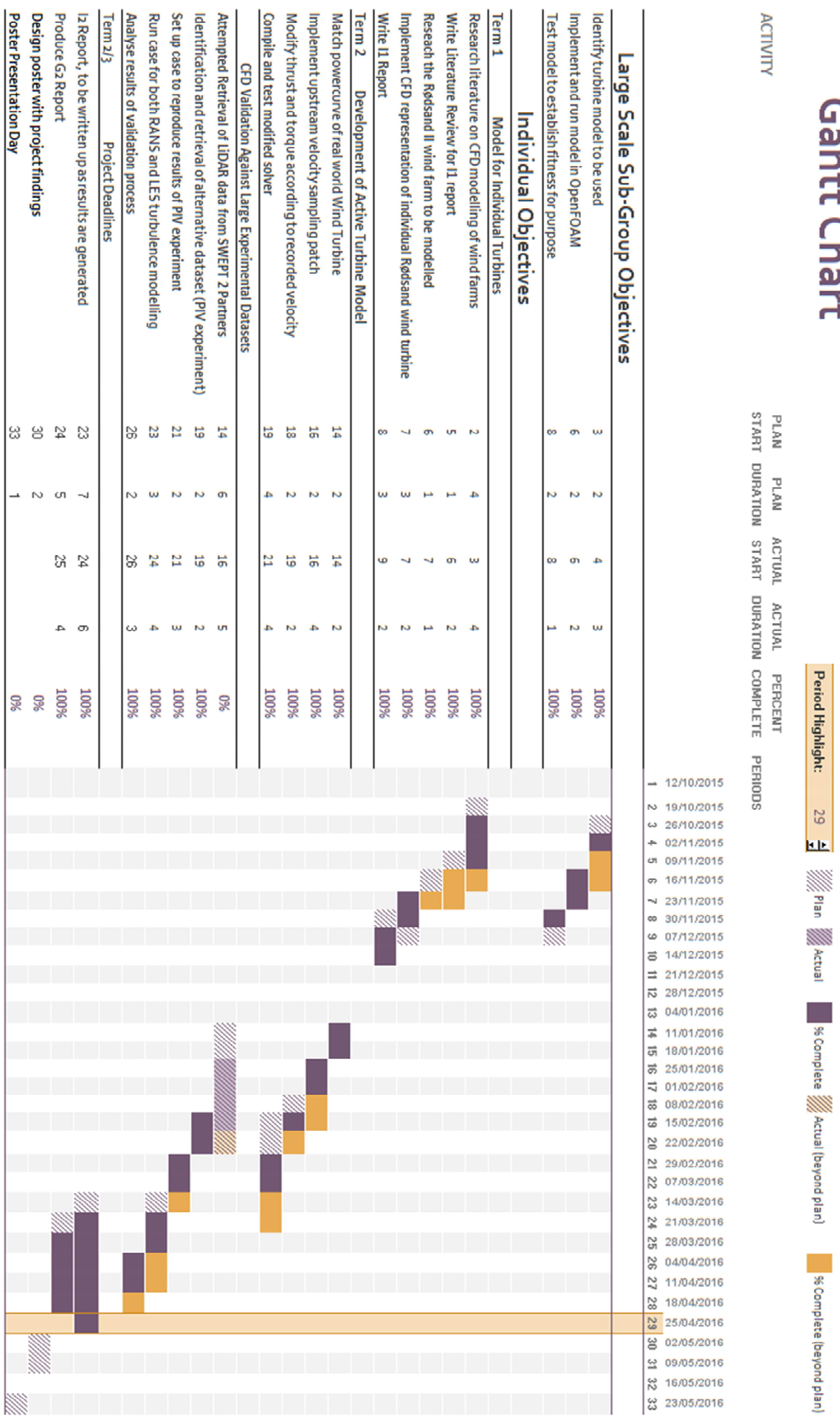


Figure 25: Gantt chart illustrating the progression of the project from start to completion

6.3. *Sustainability*

This project has sustainability at its core; in seeking improved modelling methodologies for the wind energy industry the project aims to contribute to the realisation of low-cost, low-carbon energy. Accurate modelling of the airflow around wind turbines allows for the design of improved wind farm layouts, increasing power yield and lowering costs.

Although CFD is computationally expensive, consuming large amounts of electricity, modelling scenarios in advance saves time, energy and resources in the long term.

6.4. *Health and Safety*

The majority of the work carried out over the course of this project was done at a computer, where risks to health and safety can be less apparent. Throughout the project duration, an effort was made to ensure that display screens were set to appropriate heights, office chairs were supportive and set to a suitable height, and that regular breaks were taken to alleviate the risks of fatigue in line with the official government guidelines for office work (Health and Safety Executive, 2013).

The PIV practical experiment made use of a high powered class 4 laser, and so was carried out by trained lab technicians at the University to minimise the risk to health.

7. Contribution to group function

This section details the various levels of interaction with other group members that occurred over the course of this project. Firstly, the management of the project and contributions to shared targets is detailed. This is followed by more specific examples of collaboration with other team members.

7.1. *General Contributions*

Weekly meetings with other team members provided an opportunity for all team members to interact and collaborate on aspects of the project. The management responsibilities were shared between members, with the roles of meeting chair and minute taker assigned via a rota. This ensured all members engaged in the project, and increased the interaction between individual members.

While writing group reports I have taken a leading role in the time management and structuring of the reports, helping to ensure the reports have come together in time for the deadlines. To perform this role, I interacted with all members of the team to ensure the report writing responsibilities were tackled as a team.

Together with Matt Howard and George Hyde-Linaker I produced a poster detailing the OpenFOAM work carried out in this project which was displayed at '*The Fourth UK & Eire FOAM and OpenFOAM® User Meeting*' which took place at the University of Exeter in April.

7.2. *Actuator Modelling of Wind Turbines in OpenFOAM*

When setting up the actuator disk model for the Siemens SWT-2.3-93 wind turbine, I worked with Tom March to set up the test case and find the turbine characteristics such as thrust and torque for the optimal wind velocity of 13.5ms^{-1} . Together we extended this approach to consider a simple array of 20 turbines.

Following this I worked with Matt Howard and George Hyde-Linaker on the calculation of the power yield of turbine models, helping them to implement a control volume approach to return turbine power.

7.3. *Upstream Sampling to set Turbine Characteristics*

The modification of the actuator disk solver to include upstream sampling was carried out together with Ben Johnson, who is seeking to implement a similar velocity sampling technique in the OpenFOAM turbine modelling toolkit he has implemented in his individual project. The results of this modification have been fed back to him, along with the modified solver to aid in his inclusion of the sampling strategy.

References

- 4C Offshore, 2012. *Rødsand 2 Offshore Wind Farm*. [Online] Available at: <http://www.4coffshore.com/windfarms/r%C3%B8dsand-2-denmark-dk11.html> [Accessed 27 November 2015].
- Abdi, H., 2007. RV and Congruence Coefficients. In: N. Salkind, ed. *Encyclopedia of Measurement and Statistics*. Thousand Oaks: Sage, pp. 849-853.
- Ashby, B., 2015. *An Actuator Disk Approach to Tidal Farm Simulation and Optimisation in OpenFOAM*, Exeter: Thesis submitted to the University of Exeter.
- Ashby, B., 2015. *II Report: Wind Farm Modelling*, Exeter: University of Exeter.
- Barthelmie, R. et al., 2005. Comparison of Wake Model Simulations with Offshore Wind Turbine Wake Profiles Measured by Sodar. *Journal of Atmospheric and Oceanic Technology*, Volume 23, pp. 888-901.
- Butler, J. & Quail, F., 2012. *Comparison of a 2nd Generation LiDAR Wind Measurement Technique with CFD Numerical Modelling in Complex Terrain*, Glasgow: University of Strathclyde.
- Castellani, F. et al., 2013. A practical approach in the CFD simulation of off-shore wind farms through the actuator disc technique. *Energy Procedia*, Volume 35, pp. 274-284.
- CFD Direct, 2015. *OpenFOAM User Guide: 6.6 Sampling data*. [Online] Available at: <http://cfd.direct/openfoam/user-guide/sample/> [Accessed 17 January 2016].
- Clark, N. & Ma'ayan, A., 2011. Introduction to Statistical Methods to Analyze Large Data Sets: Principal Components Analysis. *Sci Signal*, 4(190), pp. 212-215.
- Dantec Dynamics, 2013. *Particle Image Velocimetry (PIV)*. [Online] Available at: <http://www.dantecdynamics.com/particle-image-velocimetry> [Accessed 2 March 2016].
- Douglas, J., Gasiorek, J., Swaffield, J. & Jack, L., 2005. *Fluid Mechanics*. 5th ed. New Delhi : Pearson.

- EPSRC, 2015. *SWEPT 2 Research Grant*. [Online]
Available at: <http://gow.epsrc.ac.uk/NGBOViewGrant.aspx?GrantRef=EP/N508500/1>
[Accessed 16 November 2015].
- Gelman, A. et al., 2013. *Bayesian Data Analysis*. 3rd ed. Boca Raton: CRC Press.
- Goldstein, S., 1929. On the Vortex Theory of Screw Propellers. *Proceedings of the Royal Society of London. Series A, Containing Papers of a Mathematical and Physical Character*, 21 January, pp. 440-465.
- González-Longatt, F., Wall, P. & Terzija, V., 2012. Wake effect in wind farm performance: Steady-state and dynamic behavior. *Renewable Energy*, 39(1), pp. 329-338.
- Health and Safety Executive, 2013. *Display Screen Equipment (DSE)*. [Online]
Available at: <http://www.hse.gov.uk/index.htm>
[Accessed 28 April 2015].
- Herp, J., Poulsen, U. & Griener, G., 2015. Wind farm power optimization including flow variability. *Renewable Energy*, Volume 81, pp. 173-181.
- Horlock, J., 1978. *Actuator Disk Theory: Discontinuities in Thermo-Fluid Dynamics*. New York: McGraw-Hill International Book Company.
- Jeromin, A., Bentamy, A. & Schaffarczyk, A., 2013. *Actuator Disk Modeling of the Mexico Rotor with OpenFOAM*. s.l., ITM Web of Conferences.
- Josse, J., Pagès, J. & Husson, F., 2008. Testing the significance of the RV coefficient. *Computational Statistics and Data Analysis*, Volume 53, pp. 82-91.
- Josse, J., Pagès, J. & Husson, F., 2008. Testing the significance of the RV coefficient. *Computational Statistics and Data Analysis*, Volume 53, pp. 82-91.
- Kulunk, E., 2011. *Fundamental and Advanced Topics in Wind Power*. 1st ed. Rijeka: InTech.
- Lane, D., 2012. *Introduction to Linear Regression*. [Online]
Available at: <http://onlinestatbook.com/2/regression/intro.html>
[Accessed 12 March 2016].

Lignarolo, L. et al., 2016. Validation of four LES and a vortex model against stereo-PIV measurements in the near wake of an actuator disc and a wind turbine. *Renewable Energy*, Volume 94, pp. 510-523.

MacKay, D., 2008. *Sustainable Energy: Without the Hot Air*. 1st ed. Cambridge: Cambridge University Press.

Magnusson, M. & Smedmen, A., 1999. Air flow behind wind turbines. *Journal of Wind Engineering*, Volume 80, pp. 169-189.

MathWorks, 2016. *corr2*. [Online]

Available at: <http://uk.mathworks.com/help/images/ref/corr2.html>

[Accessed 8 March 2016].

Odemark, Y. et al., 2009. *High-Cycle Thermal Fatigue in Mixing Tees: New Large-Eddy Simulations Validated Against New Data Obtained by PIV in the Vattenfall Experiment*. Brussels, ASME.

Piomelli, U. & Balaras, E., 2002. Wall-layer models for large-eddy simulations. *Annual Review of Fluid Mechanics*, 34(1), pp. 349-374.

Pointwise, 2011. *T-Rex Hybrid Meshing in Pointwise*. [Online]

Available at: <http://www.pointwise.com/theconnector/July-2011/T-Rex-Hybrid-Meshing-in-Pointwise.shtml>

[Accessed 18 March 2016].

Pointwise, 2016. *Compute Grid Spacing for a Given Y+*. [Online]

Available at: <http://www.pointwise.com/yplus/>

[Accessed 5 March 2016].

Porté-Agel, F., Wu, Y.-T. & Chen, C.-H., 2013. A Numerical Study of the Effects of Wind Direction on Turbine Wakes and Power Losses in a Large Wind Farm. *Energies*, Volume 6, pp. 5297-5313.

Robert, P. & Escoufier, Y., 1976. A Unifying Tool for Linear Multivariate Statistical Methods: The RV- Coefficient. *Journal of the Royal Statistical Society. Series C (Applied Statistics)*, 25(3), pp. 257-265.

Sheng, J., Meng, H. & Fox, R., 1998. Validation of CFD simulations of a stirred tank using particle image velocimetry data. *The Canadian Journal of Chemical Engineering*, 76(3), pp. 611-625.

Svenning, E., 2010. *Implementation of an actuator disk in OpenFOAM*, Gothenburg: Chalmers University of Technology.

Wu, Y.-T. & Porté-Agel, F., 2013. Simulation of Turbulent Flow Inside and Above Wind Farms: Model Validation and Layout Effects. *Boundary-Layer Meteorology*, 146(2), pp. 181-205.